Supplementary Information: Therapeutic peptide delivery via aptamer-displaying, disulfide-linked peptide amphiphile micelles

Josiah D. Smith[1*], Leah N. Cardwell[2*], David Porciani[2], Andrea Nolla[1], Brenna Cornelison[1], Megan Schulte[1], Fabio Gallazzi[3,4], Donald H. Burke[2,5], Mark A. Daniels[2,6], and Bret D. Ulery[1,#]

[1]Department of Biomedical, Biological, and Chemical Engineering, University of Missouri, Columbia, MO
[2]Department of Molecular Microbiology and Immunology, University of Missouri, Columbia, MO
[3]Department of Chemistry, University of Missouri, Columbia, MO
[4]Molecular Interactions Core, University of Missouri, Columbia, MO
[5]Division of Biochemistry, University of Missouri, Columbia, MO
[6]Department of Surgery, University of Missouri, Columbia, MO
Corresponding author
* Co-first authors

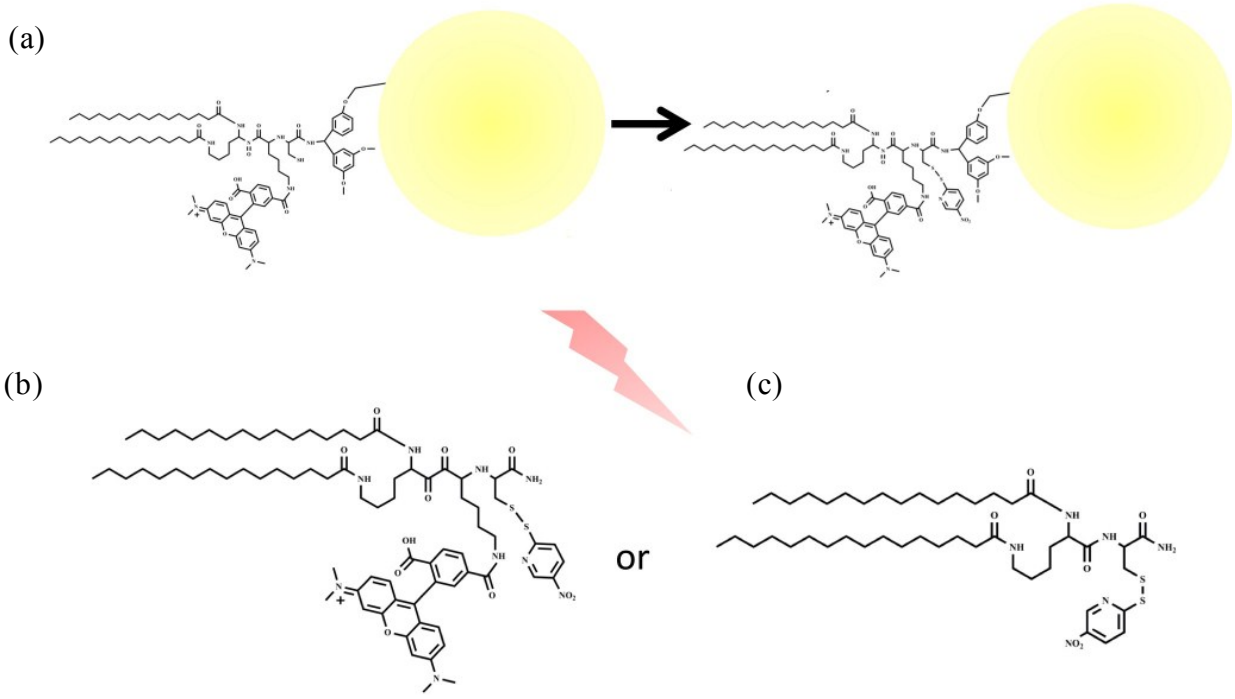

Scheme S1: Solid-phase activated lipid synthesis. The yellow circle represents a rink amide resin bead as the solid-phase support on which the lipid is synthesized. (a) This reaction shows the activation of the cysteine side chain thiol of dipalmitoyllysyllysyl(tetramethylrhodamine)cysteine ($Palm_2$K-K(TAMRA)-C) lipid by 3-nitro-2-pyridinesulfenyl (Npys) for which (b) trifluoroacetic acid-mediated cleavage from resin yields $Palm_2$K-K(TAMRA)-C(Npys). (c) Fluorophore-free, therapeutic lipid can be synthesized by the synthesis of $Palm_2$K-C(Npys).

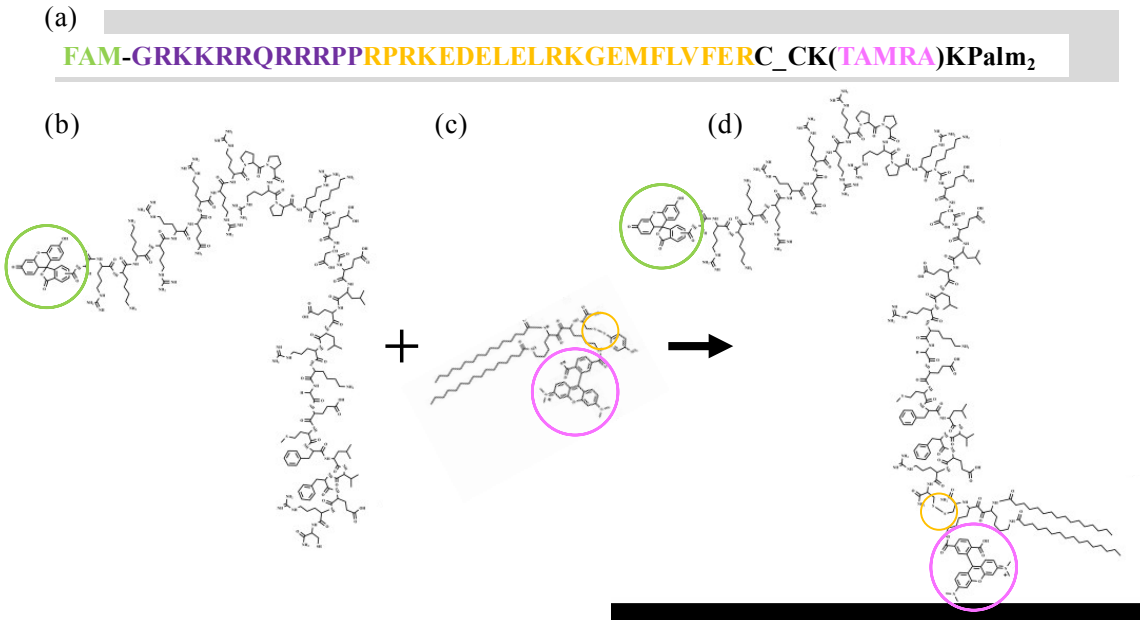

Scheme S2: POSH peptide amphiphile synthesis. (a) The peptide amino acid sequence is provided with FAM and TAMRA fluorophores in green and pink, respectively. The Tat portion of the peptide is shown in purple and the POSH portion in gold. (b) FAM-Tat-POSH-C and (c) $Palm_2$KK(Tamra)C(Npys) were joined by sulfide to sulfide conjugation with FAM, TAMRA, and disulfide linkage circled in green, pink, and yellow, respectively. The reaction was completed overnight in dimethylformamide (DMF) at ~20 mg/mL with a 1.5x molar excess of $Palm_2$KK(Tamra)C(Npys). For the reaction, the reaction was observed visually via the development of a bright yellow color consistent with Npys displacement. PAs were dried via rotary evaporation and purified by HPLC prior to further use.

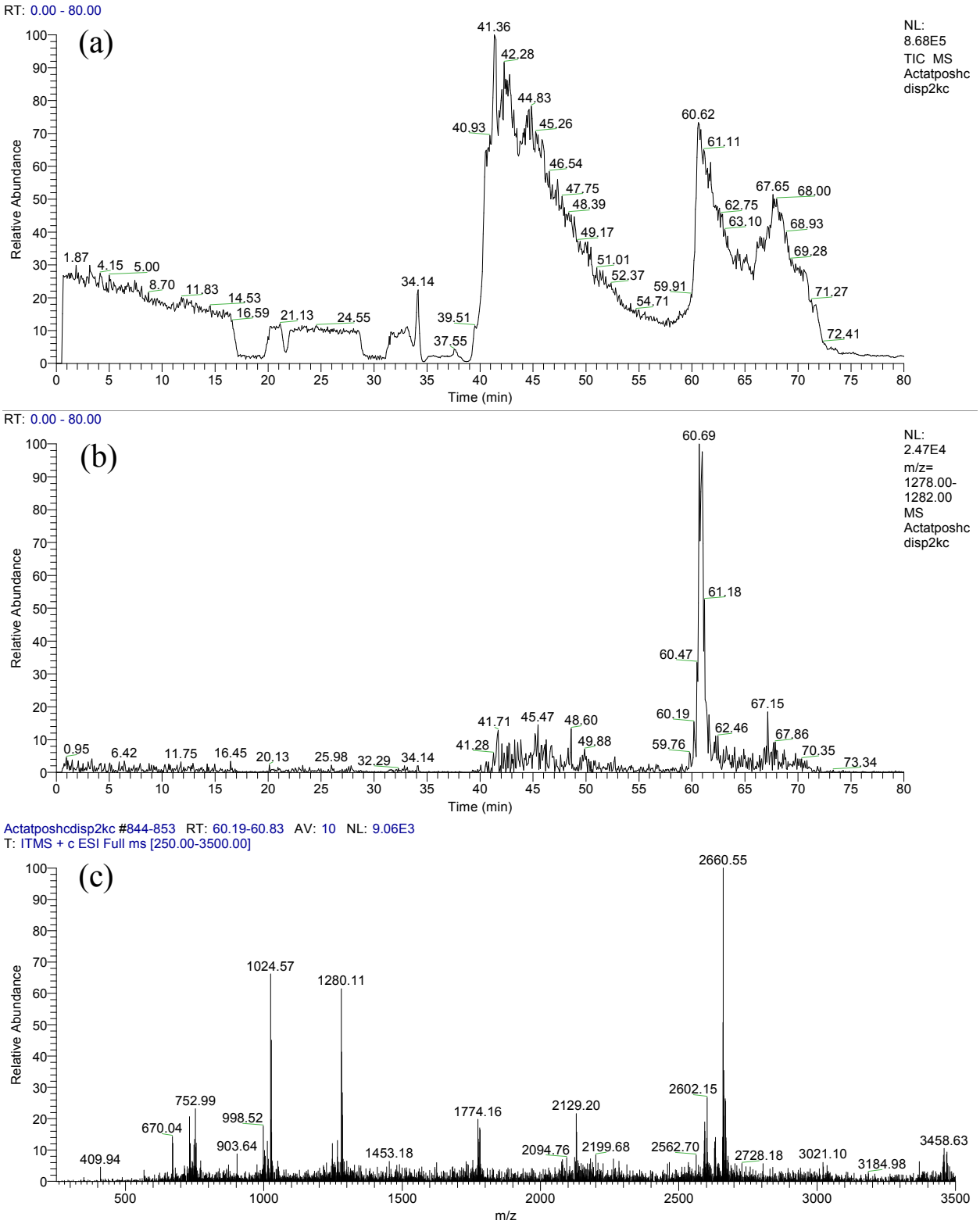

Figure S1: Tat-POSH-C_CKPalm$_2$ purification. (a) The total ion count spectrum and (b) target ion peak within the spectrum (~ 1280 Da) throughout the 80 minute purification process is shown. (c) The observed M/Z data at ~ 60.5 minutes confirms that the product molecular weight is as expected based on the constitutive amino acids.

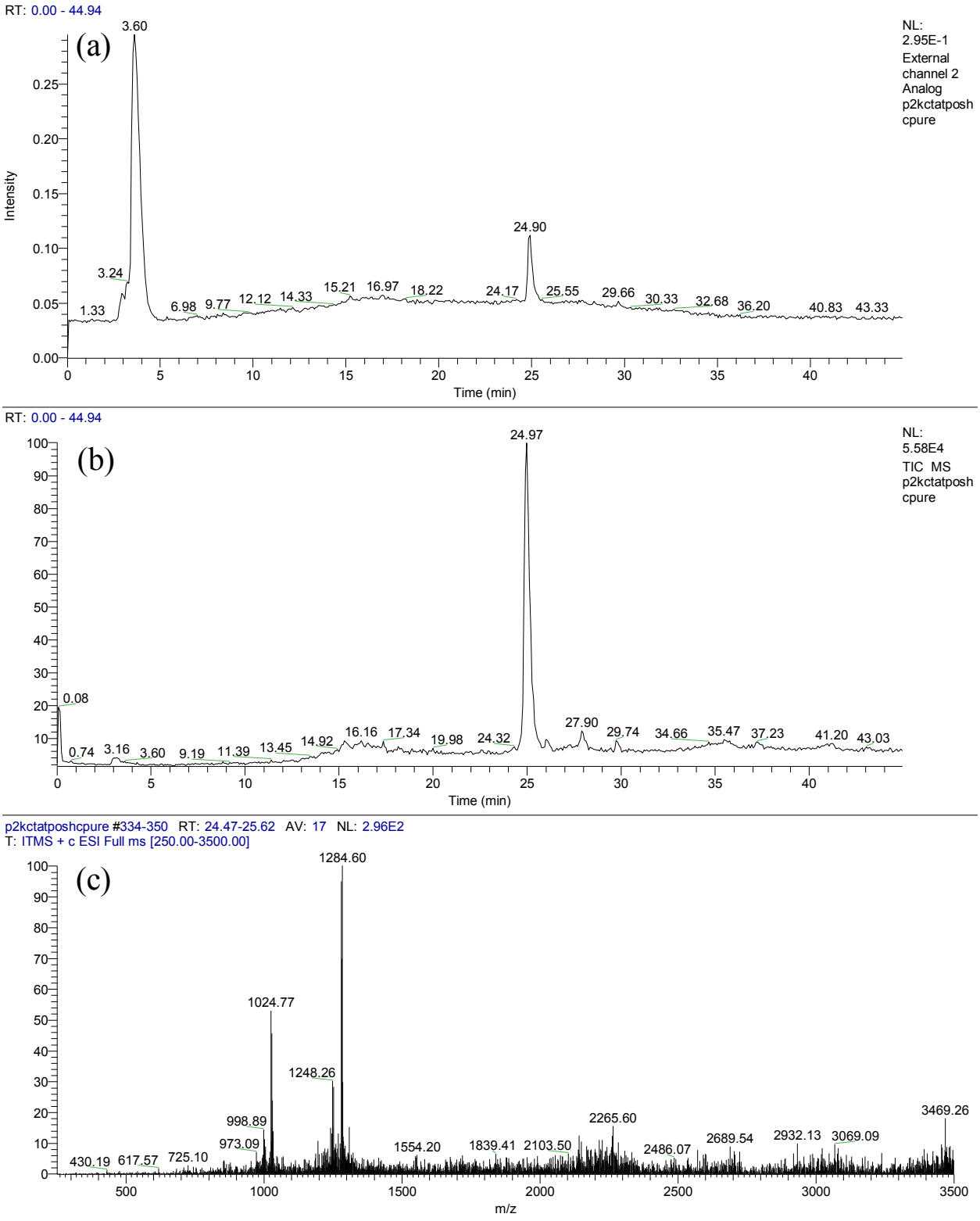

Figure S2: Purified Tat-POSH-C_CKPalm$_2$ analysis. (a) The LC absorbance spectrum at 214 nm and (b) total ion count spectrum through the 30 minute analysis shows a highly pure product eluted at 24.9 - 25 minutes. (c) The observed M/Z data at ~ 25 minutes confirms the product molecular weight (~ 1280 Da) in high purity verifying successful purification.

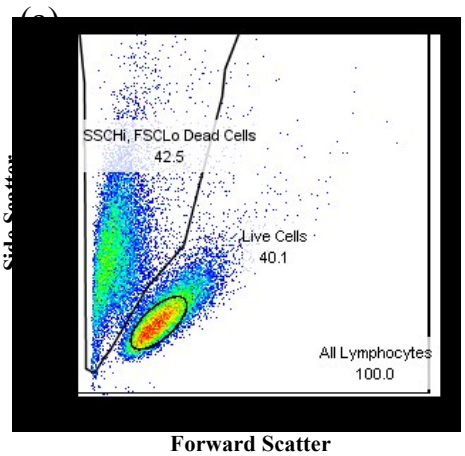

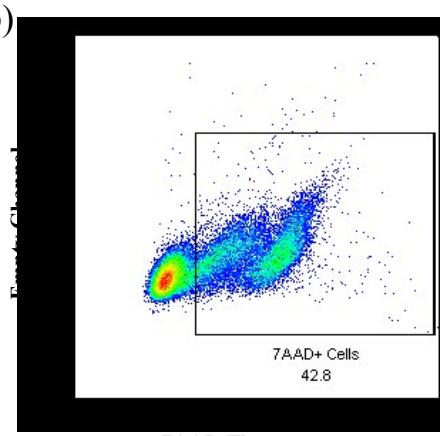

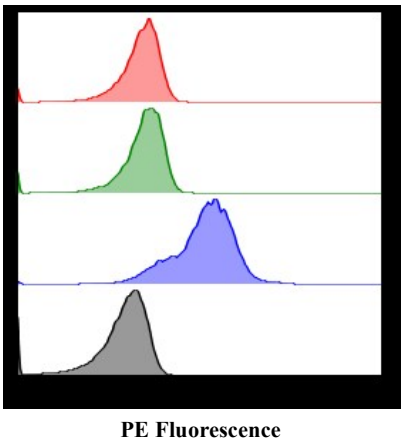

Color	Formulation	MFI
Red	scApt~Antitail-Cy3	131
Green	G24A~Antitail-Cy3	144
Blue	C10.36~Antitail-Cy3	984
Black	Untreated	75.5

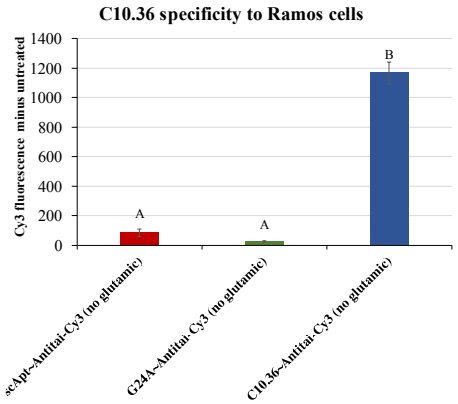

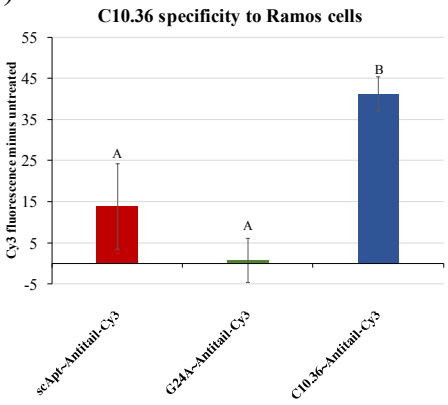

Figure S3: Flow cytometry data analysis. (a) Dead cells were identified by side scatter / forward scatter population evaluation and (b) confirmed via 7-AAD staining. (c) phycoerythrin (PE) histograms show the fluorescent intensity of lymphocyte population when using Cy3 and TAMRA fluorophores. (d) MFI (Cy3 or TAMRA) was utilized to compare experimental groups with aptamer association shown here in a representative example. Flow was used to investigate aptamers annealed to Cy3-labeled antitail incubated using the standard 10-minute procedure. MFI plots for aptamers in cell incubation conditions (e) similar to previously reported results (*i.e.* aptamer without glutamic acid) and (f) optimized for micelles (*i.e.* aptamer with glutamic acid). Groups with different letters have statistically different values as determined by Tukey-HSD with an $\alpha = 0.05$.

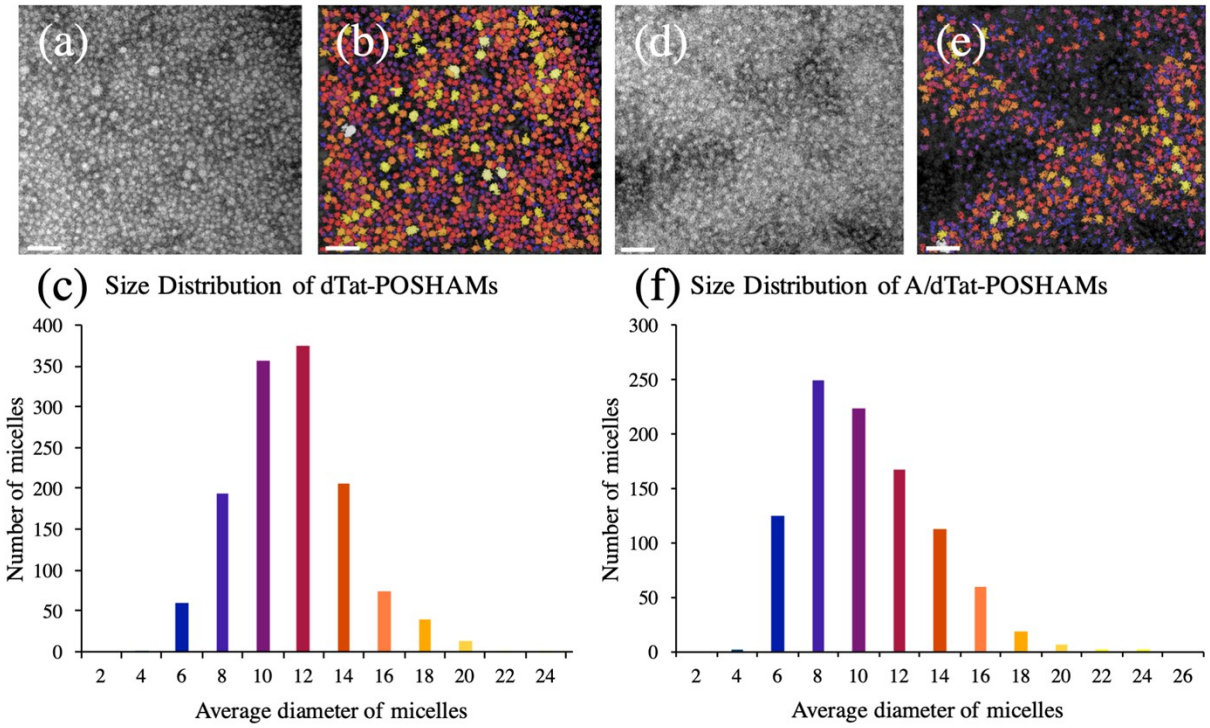

Figure S4: Micelle size analysis. Representative TEM micrographs for A/dTat-POSHAMs and dTat-POSHAMs are given with the corresponding size analysis "heatmap" overlay and histogram. (a) - (c) A/dTat-POSHAMs are shown in the left panel, including (a) a TEM micrograph, (b) a TEM analysis "heatmap", and (c) a histogram. (d) - (f) Similar data for dTat-POSHAMs are likewise shown in the right panel. The "heatmap" was produced using the Bruker ESPRIT 2.1 software package. Each analysis required the independent optimization of the analytical method by adjusting micrograph brightness, contrast, and circularity requirements, as well as by altering the size-range of nanoparticles expected. Care was taken to review each analysis after the fact using direct close side-by-side inspection for consistency with the original micrograph. Scale bars are 50 nm.

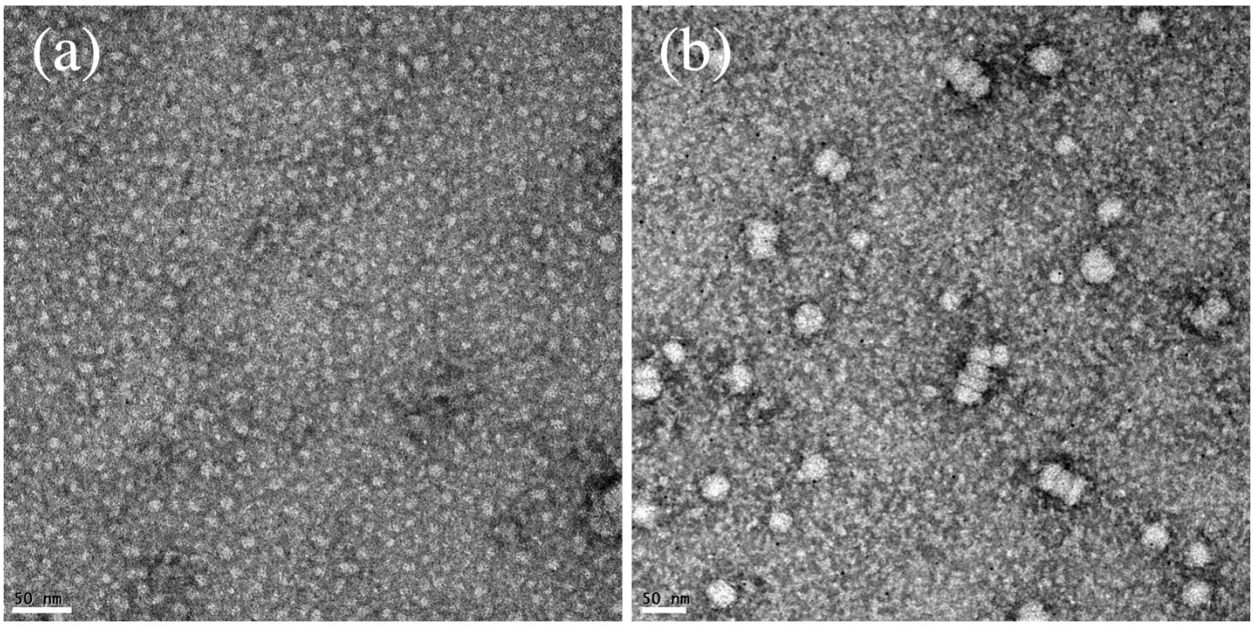

Figure S5: C10.36~A/dTat-POSHAM FBS-mediated micelle disassembly resistance. (a) Individual micelles before FBS exposure exist as spherical nanoparticles. (b) Upon incubation with 10% FBS in PBS at 37 °C for 1 hour, micelles appear slightly larger, but retain their spherical structure with limited evidence of disassembly. The scale bar for each panel is 50 nm.

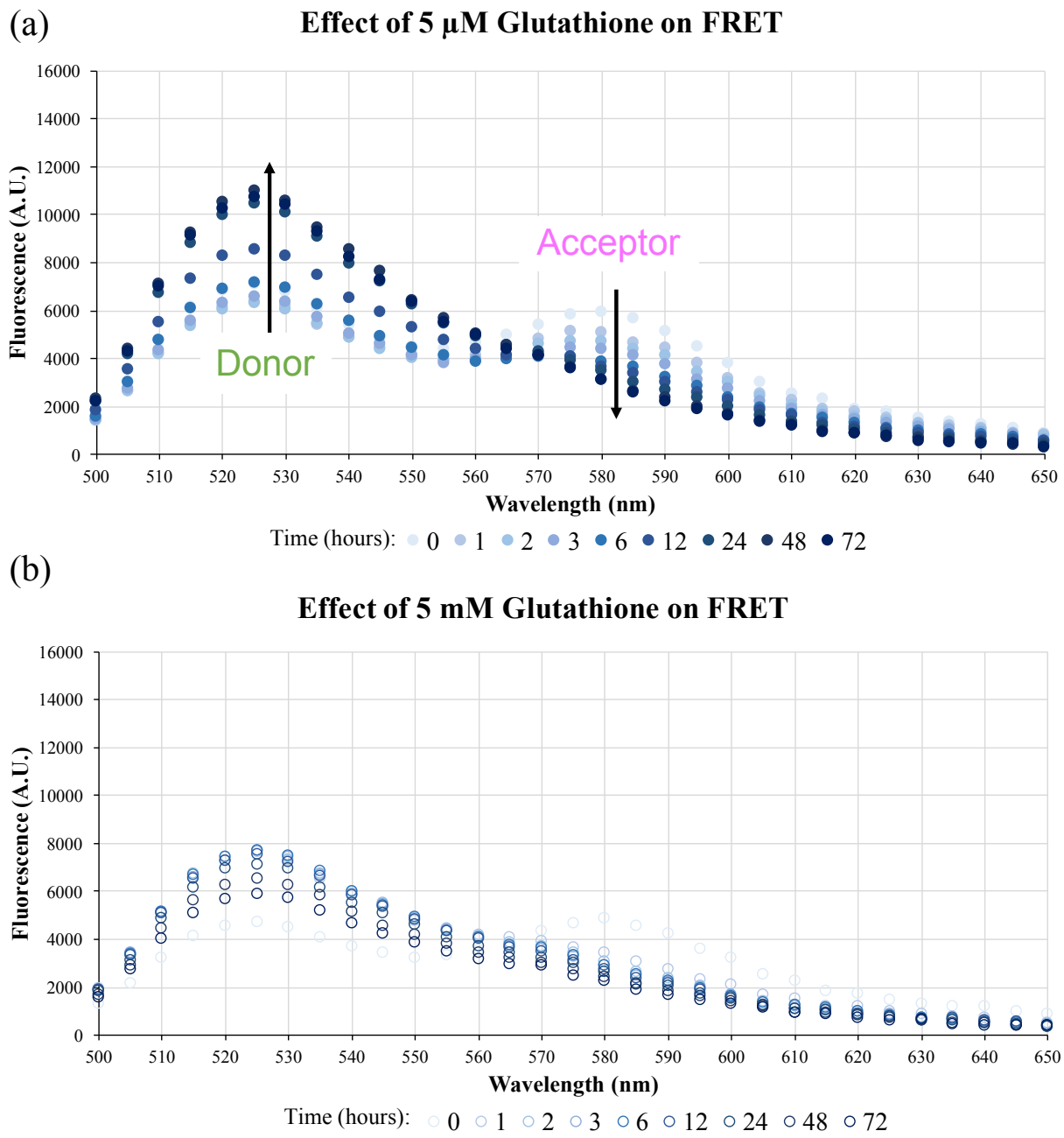

Figure S6: Glutathione-mediated disulfide bond cleavage. FRET of dual-fluorophore labeled dPA in C10.36~A/dTat-ScramAMs diminishes (*i.e.* donor at 525 nm increases and acceptor at 585 nm decreases) over 72 hours indicating peptide-lipid separation in the presence of (a) 5 µM and (b) 5 mM glutathione. With 5 µM glutathione, C10.36~A/dTat-ScramAMs possessed less FRET at each time point over 72 hours. By comparison, C10.36~A/dTat-ScramAMs exposed to 5 mM glutathione reached peak donor fluorescence at ~ 6 hours likely attributed to the maximum number of disulfide bonds having been broken at that time point.

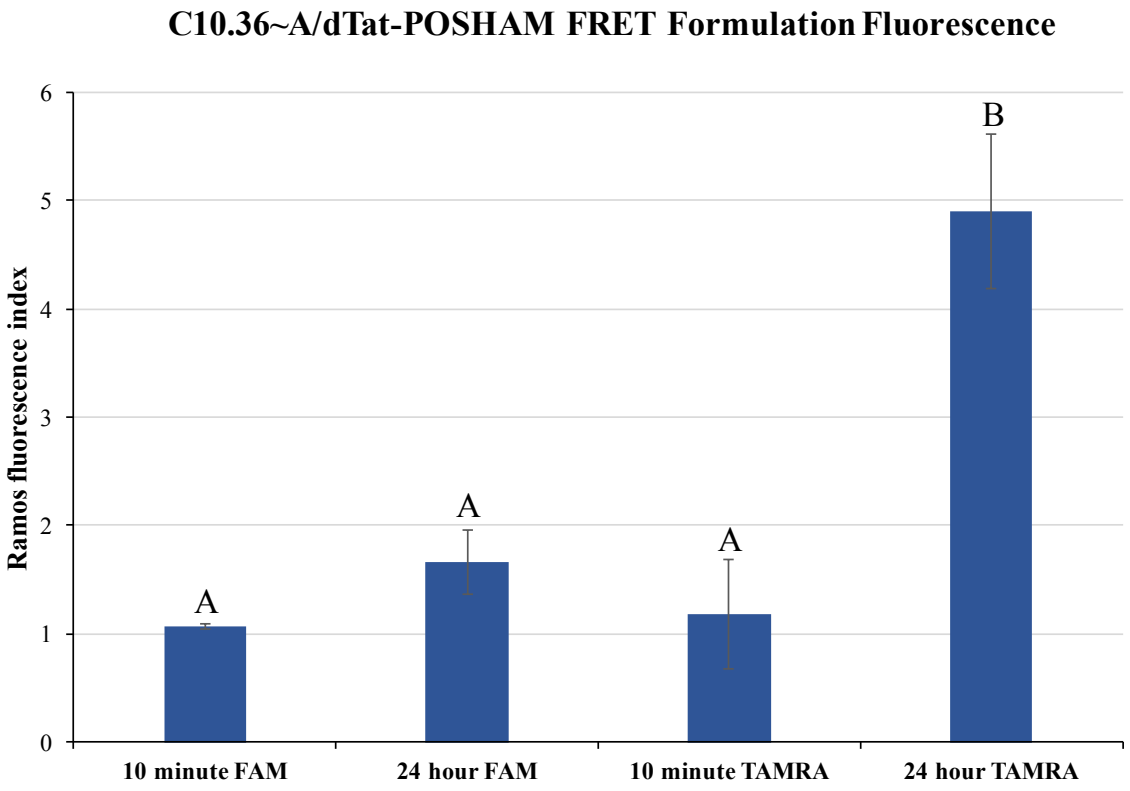

Figure S7: C10.36~A/dTat-POSHAM fluorescence change during Ramos treatment. FAM and TAMRA fluorescence were evaluated via flow cytometry after 10 minutes of incubation followed by immediate assessment or after 24 hours of cell culture and indexed against untreated Ramos cells. Both FAM and TAMRA increased in fluorescence after culturing, but the change for TAMRA was much greater in magnitude and more consistent with expected micellar disassembly. Groups with different letters have statistically different means (Tukey HSD, $\alpha = 0.05$).

Table S1: Aptamer and antitail DNA sequences. The underlined portion of C10.36, G24, and scApt demarcate the "tail" sequence for anealing to antitail. The underlined portion of sctC10.36 is the modified "tail" sequence unable to anneal to antitail. All sequences are listed 5' to 3'.

C10.36	CTAACCCCGGGTGTGGTGGGTGGGCAGGGGGGTTAGCGACGACGACGACGACGACGACGA
sctC10.36	CTAACCCCGGGTGTGGTGGGTGGGCAGGGGGGTTAGTAGTCGTAGTCGTAGTCGTAGTCGTAG
G24A	CTAACCCCGGGTGTGGTGGGTGG**A**CAGGGGGGTTAGCGACGACGACGACGACGACGACGA
scApt	GCCATTGCCATTGCCATTGCCATTGCCATTGCCATTGCCATTGCCATTGCCATTGCGACGACGACGACGACGACGACGA
antitail	TCGTCGTCGTCGTCGTCGTCG

Table S2: CD spectra analysis. Data for each formulation showed an increase in ß-sheet conformation and decrease in random coil conformation compared to Tat-POSH-C.

Structure	**Tat-POSH-C**	**dTat-POSHAMs**	**A/dTat-POSHAMs**	**G24A~A/dTat-POSHAMs**	**C10.36~A/dTat-POSHAMs**
α-helix	0%	0%	0%	2%	0%
β-sheet	36%	48%	47%	45%	47%
Random coil	64%	52%	53%	53%	54%